coasts

MDPI

Article

Wind as an Influential Factor in the Transport and Destination of Oil from Spills Along the Brazilian Semiarid Coast (Ceará State, Northeast Brazil)

Alexandre Medeiros de Carvalho [1,2], Lidriana de Souza Pinheiro [1,2,3], Antonio Rodrigues Ximenes Neto [4], Vanda Claudino-Sales [5,*], Sérgio Rossi [1,2,3], José Francisco Soares Lima Júnior [6,†], Regimario Pereira Lima Filho [1,2], Beatriz Diniz Lopes [1,2], Thalya dos Santos Sousa [1,2] and Rivelino Martins Cavalcante [1,2]

1 Geological Oceanography Laboratory (LOG), Institute of Marine Sciences-LABOMAR—Federal University of Ceará (UFC), Fortaleza 60165-081, CE, Brazil; medeiros@ufc.br (A.M.d.C.); lidriana@ufc.br (L.d.S.P.); sergio.rossi@unisalento.it (S.R.); regimario@alu.ufc.br (R.P.L.F.); thalyasantos@alu.ufc.br (T.d.S.S.); rivelino@ufc.br (R.M.C.)
2 Marine Ecology and Conservation Laboratory (MARES), Institute of Marine Sciences-LABOMAR—Federal University of Ceará (UFC), Fortaleza 60165-081, CE, Brazil
3 Department of Biological and Environmental Sciences and Technologies (DiSTeBA), Università del Salento, 73100 Lecce, Italy
4 Geomorphology and Applied Sedimentology Laboratory (LAGESA), Geography Department (DGC), Federal University of Rio Grande do Norte (UFRN), Caicó 59300-000, RN, Brazil; antonio.ximenes@ufrn.br
5 Geography Graduation Program, Federal University of Pelotas (UFPEL), Pelotas 96010-770, RS, Brazil
6 Coastal and Oceanic Geology and Geomorphology Laboratory (LGCO), Geography Course, State University of Ceará (UECE), Fortaleza 60714-903, CE, Brazil
* Correspondence: vcs@ufc.br
† In memoriam.

Abstract

Oil spills along the northeast coast of Brazil have the potential to cause catastrophic contamination of coastal environments and their associated biota. Beyond the direct contamination processes occurring on beaches, oil can also be transported inland by tides through estuaries. In addition, wind-driven transport of oil was observed in nearly all sections studied along the coast. Therefore, this study evaluated the potential of wind to transport oil fragments inland using both direct and indirect methods, including field observations and GIS-based mapping tools. The results identified and quantified oil fragmentation processes and wind-driven transport over relatively large distances (hundreds of meters). The presence of exhumed beachrock, combined with the absence or low elevation of foredunes and the high potential for wind transport, plays a crucial role in trapping oil on the beach surface. These factors further facilitate the fragmentation and inland dispersal of oil particles, allowing them to penetrate deeper into the coastal environment. The findings underscore the importance of assessing the contamination risks posed by oil fragments as they become incorporated into aeolian and other interconnected inland systems.

Keywords: oil spill; beach; wind action; environment

Check for updates

Academic Editor: Muk Chen Ong

Received: 1 November 2025
Revised: 28 February 2026
Accepted: 1 April 2026
Published: 9 April 2026

1. Introduction

Oil spills on the world's coasts have been a recurrent problem. Examples include the Madagascar oil spill (Madagascar Island), the RFA Darkdale wreck (St. Helena, British Territory), the Gulf oil spill (Arabian Gulf), the Solar I oil spill (Guimaras Island, Philippines), the Husky oil spill (Saskatchewan, Canada), and the infamous "Deepwater Horizon" spill (Gulf of Mexico) [1–6].

Between August 2019 and March 2020, beaches along the Brazilian coast were impacted by an oil spill exceeding 5000 tons, contaminating over 3000 km of coastline [7–9]. Due to the geographic extent of the oil spreading and its social, economic, and ecological impacts, it is considered the largest oil spill off the coast of South America and other tropical environments [7,9].

According to Reddy et al. [10], the oil was identified as fuel oil, rather than crude oil as previously believed, and it was confirmed to have a high chemical similarity to oil from the Venezuelan Basin. The migration dynamics of this oil from its presumed origin, along with its behavior as it dispersed along this vast coastal region, has been the focus of numerous studies [4,11]. In this case, the oil's movement was closely associated with marine currents, wave dynamics, and coastal drift [12]. Additionally, factors such as wind action, beach types, and intertidal rocks are crucial for understanding and predicting the displacement and fixation of oil along the coast [13]. The role of wind in transporting oil from the beach face to inland aeolian landscapes, as well as its impact on oil dispersion and environmental contamination, has been less frequently studied.

On the coast of Ceará, the agents responsible for oil transport, particularly waves and currents, have been the focus of research [12]. This research provides a reasonably accurate explanation of how oil contaminates certain areas of the coastline where wind action is strong and recurrent. However, the oil's permanence or dispersion is also influenced by the materials that make up the coastal environment and their effect on local morphodynamics. Evidence that winds can transport oil fragments, becoming part of the coastal aeolian morphology and contaminating environments under wind influence, underscores the need to assess wind's impact on the diverse life forms in these areas.

Understanding the role of wind in transporting oil is essential for predicting where oil may accumulate and how it might interact with the environment. In this study, the distribution of oil along the coast following the 2019 oil spill was examined first, evaluating also the contribution of coastal dynamics to the dispersion and fixation of the material.

2. Study Site

The study area along the Equatorial Northeast Brazilian coast (Figure 1) falls under a tropical semiarid climate [14], influenced by a sub-humid tropical climate, with a rainy season from January to May and a dry season from June to December. The region receives about 1400 mm of rainfall annually, with an average temperature of 27 °C and low temperature variation [15].

Most of the time, the dynamics of the northeastern coast are controlled by sea-type waves, but dispersive waves, or swells, also play a significant role [16–18]. The tidal regime is characterized by a semidiurnal and mesotidal system, subjected to a tidal variation range of 2 to 3 m, on neap tide and spring tide, respectively, and astronomic tides can reach maximum value of 3 m and minimum of −0.2 m [19].

The wind regime varies seasonally in an inverse relationship to the rainfall pattern [16,20,21], with lower wind speeds in the first half of the year and maximum values in the second half. The predominant wind directions are from the E and ESE quadrants, driven by southeasterly trade winds [16,22,23]. These winds are characterized as unidirectional easterly winds, with the ratio of resultant drift potential (RDP) to drift potential (DP) close to 1, and an average drift potential of about 692 v.u. [24].

https://doi.org/10.3390/coasts6020016

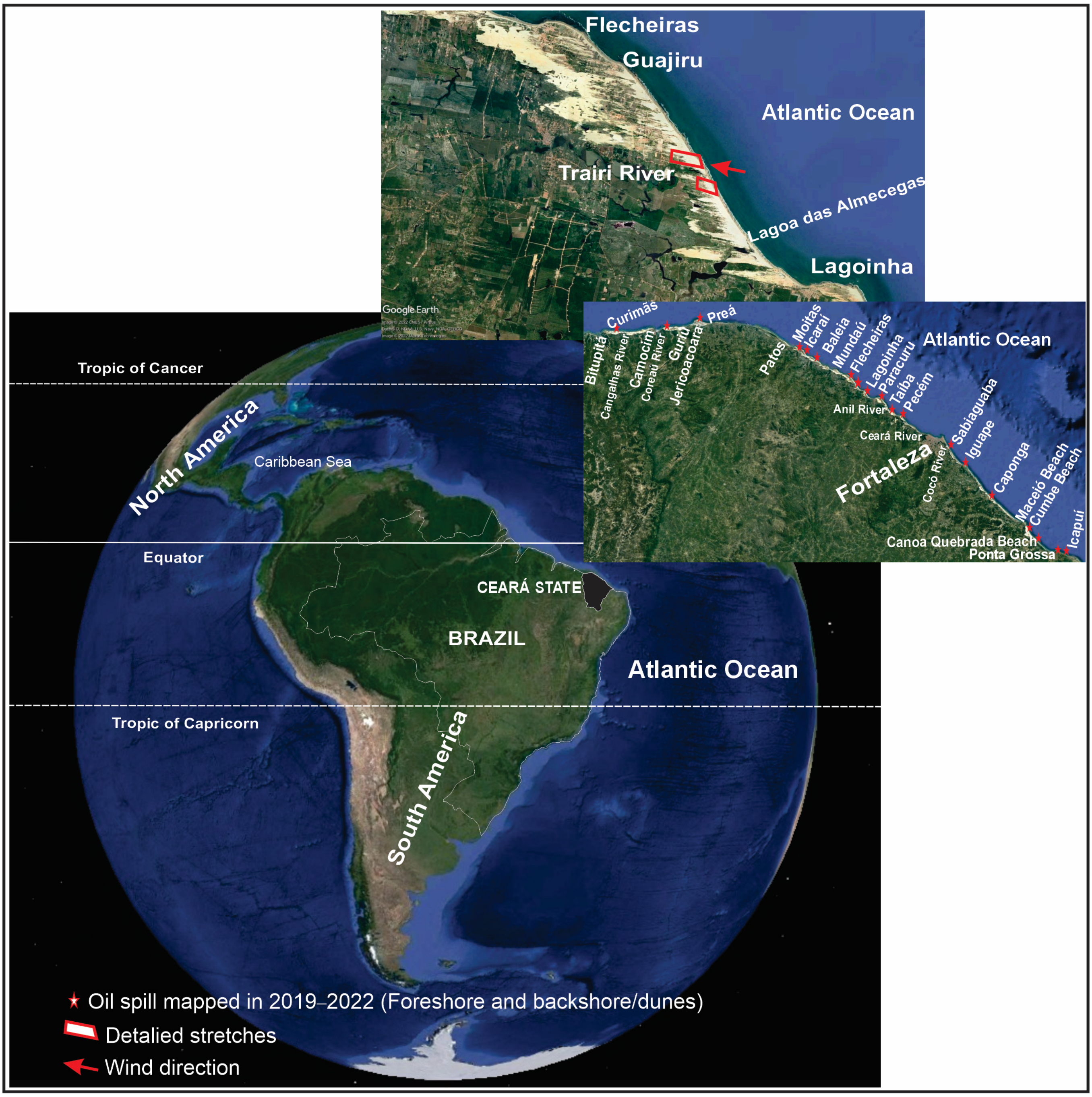

Figure 1. Study area in the Brazilian equatorial coast. In the figure it is represented as stars with red edges oil spill mapped in 2019–2022 in the coastal zone of Ceará (NE Brazil).

Under the influence of southeasterly trade winds, high-energy marine conditions occur between September and November, when the intertropical convergence zone (ITCZ) withdraws, allowing the development of intense winds. Swell events are most common between January and March [25] due to frequent low-pressure cyclonic systems over the North Atlantic, which turns the region into a major cyclogenesis zone [26,27]. These swells, generated between 35° N and 65° N, take about 3 days to reach the Northeast Brazilian coast [28]. Significant wave heights (Hs) of up to 2.8 m, peak periods (T) of 11 to 20 s, and peak directions (Dp) from NW to NE, combined with spring tide maxima resulting in heights (Hr) of up to 5 m, characterize local storm surge events [25]. The high energy associated with these events can rapidly and significantly reshape the coastal landscape, depositing or removing sediments from various beach sectors [19].

Much of this coast consists of headland–bay–beach sequences, commonly referred to as zeta-form bays [16,29,30]. These sequences are formed by rocky headlands separated by medium-to-fine quartz-rich sandy bays, which are often backed by extensive dune fields [31]. This headland–bay–beach system, with its seaward–concave plan, is influenced by wave refraction and diffraction in the shadow zones behind the headlands, resulting in varied coastline orientations [32]. The more resistant geological materials form headlands, while less resistant materials form bays. This configuration results in different sedimentological responses along the bay. Intense wave diffraction occurs near the curved bays, causing sediment to be transported by wind from the upstream headlands. In the straighter segments of the coastline, wave refraction predominates, depositing sediments more parallel to the shore, which are then available for aeolian transport inland [31].

These coastal dynamics have contributed to the formation of at least three generations of dunes along the Ceará State coastline [16,17,20], with mobile white dune fields being a dominant feature of the Northeast Equatorial coast.

In shaping the equatorial northeast coast, this headland–bay–beach–dune configuration also creates active cliffs, paleocliffs, and cliffs partially or entirely covered by aeolian deposits. In certain areas, less resistant rocks develop abrasion platforms, some of which also serve as bases for beachrock formation [16].

The coastal stretch from the Ceará River to west of the Coreaú River mouth is characterized by sandy beaches separated by headlands, forming embayments. Abrasion platforms and cliffs composed of conglomeratic–clay–ferruginous deposits from the Barreiras/Camocim Formations and Post-Barreiras sediments dominate the landscape, providing natural protection against wave action, often in association with beachrocks. Quartzite and migmatitic gneiss outcrops support headlands, especially around Jericoacoara. The region features active sandy and ferruginous cliffs, extensive beachrock platforms, mobile white dunes, and prominent aeolianites with tabular and ruiniform morphologies [33].

3. Materials and Methods

3.1. Mapping

The identification and mapping of coastal landforms were performed through remote sensing and fieldwork methods. Remote sensing was based on historical images from 2004 to 2023 using Google Earth Pro software (7.3.4, 2004). The composition and morphological patterns were validated during fieldwork conducted between June and November 2022. Figure 1 shows the sectors analyzed across approximately 600 km of the semiarid coast in the Western Equatorial Atlantic.

To conduct the study, a survey of Landsat and Copernicus satellite images from 2004 to 2023 was performed. These images were processed and georeferenced using the SIRGAS2000/UTM ZONE 24S datum in the software QGIS 2.18.23.

3.2. Morphology and Morphodynamic Analysis

The study of geomorphology and its interaction with eolian dynamics was carried out in two stages: (1) remote sensing, which evaluated wind incidence based on the shape and positioning of the coastline; and (2) fieldwork, where local geomorphology and surface structures that either impede or facilitate aeolian transport towards the continent's interior were assessed. The active aeolian morphologies, terrain surfaces, and their relationship with current dynamics were also evaluated [34].

Measurements of wind transport direction and beach slope, as well as the orientation of beachrock cross-strata, were taken using a Brunton compass and the Stereonet Mobile app for iOS v. 3.0 © [35] for iPhone.

3.3. Particle Size Analysis

Sediment samples were collected along a designated stretch, beginning at the beach and extending inland, to analyze variations in sand grain size and oil fragment distribution. Sediment samples were dried to determine grain size using the gravimetry analysis method proposed by Suguio [36]. For analysis, 100 g of each sample was wet sieved to separate the mud fraction from sand and gravel. The mud fraction was less than 10%. Grain size analysis was performed at 1 phi intervals using a mechanical agitator for 10 min at a frequency of 10 Hz. A sequence of sieves with different mesh sizes was used, following the Wentworth [37] classification.

Granulometry data and statistical parameters were obtained using the SYSGRAN 3.0 software [38]. The statistical parameters used followed the Folk and Ward [39] method, which is widely applied to beach and dune sedimentology.

3.4. Waves, Tides, Winds

The wave climate analyzed was based on the Wavewatch III model database, during the 1-year data period, in order to verify the influence of seasonality. In addition, tidal data were used from the database of the ports in the region, as made available by the Brazilian Navy, based on the spring tide amplitudes, since our focus in the work is the transfer of oil from the upper foreshore (near the high tide line) to the adjacent aeolian system. Meteorological data, such as daily precipitation rates, wind speed, and direction, were collected from an in situ sensor at the Fortaleza Meteorological Station, monitored by the National Institute of Meteorology (INMET).

4. Results

4.1. Oil Distribution on the Coast

Oil spill have been identified along approximately 19 stretches of the studied coast (Figure 1), with oil fragments passing from the beach face and reaching the incipient foredunes in about six of these areas. However, in most cases, oil fragments are retained at the base of the windward face of the incipient foredunes, as observed in Cascavel, Iguape, Pecém, Paracuru, Flecheiras, Baleia, and Jericoacoara (Figure 2).

In certain stretches, such as Bitupitá, Flecheiras/Lagoinha, and Cumbe Beach (Aracati), oil fragments are transported landward by the wind, moving far beyond the first incipient foredune ridge. At Cumbe Beach, located approximately 150 km east of Fortaleza, oil fragments are transported beyond the foredune belt, reaching more than 20 m inland from the high tide line (Figure 1). This transport occurs along an aeolian deflation surface, developed from the windward front of the first incipient foredune ridge (Figure 3). This area experiences strong wind activity and features stretches with no foredunes.

The main area of focus in this study is the beach stretches east and west of the Trairi River mouth, between Lagoinha and Flecheiras (Figure 1). On both sides, the beach has a low slope and features a large platform formed by beachrock positioned along the middle portion of the beach profile. These beachrocks along the studied coast are often exhumed and serve as structural barriers or traps, restricting the free flow of sediments and oil to offshore areas during tidal changes and storm surges.

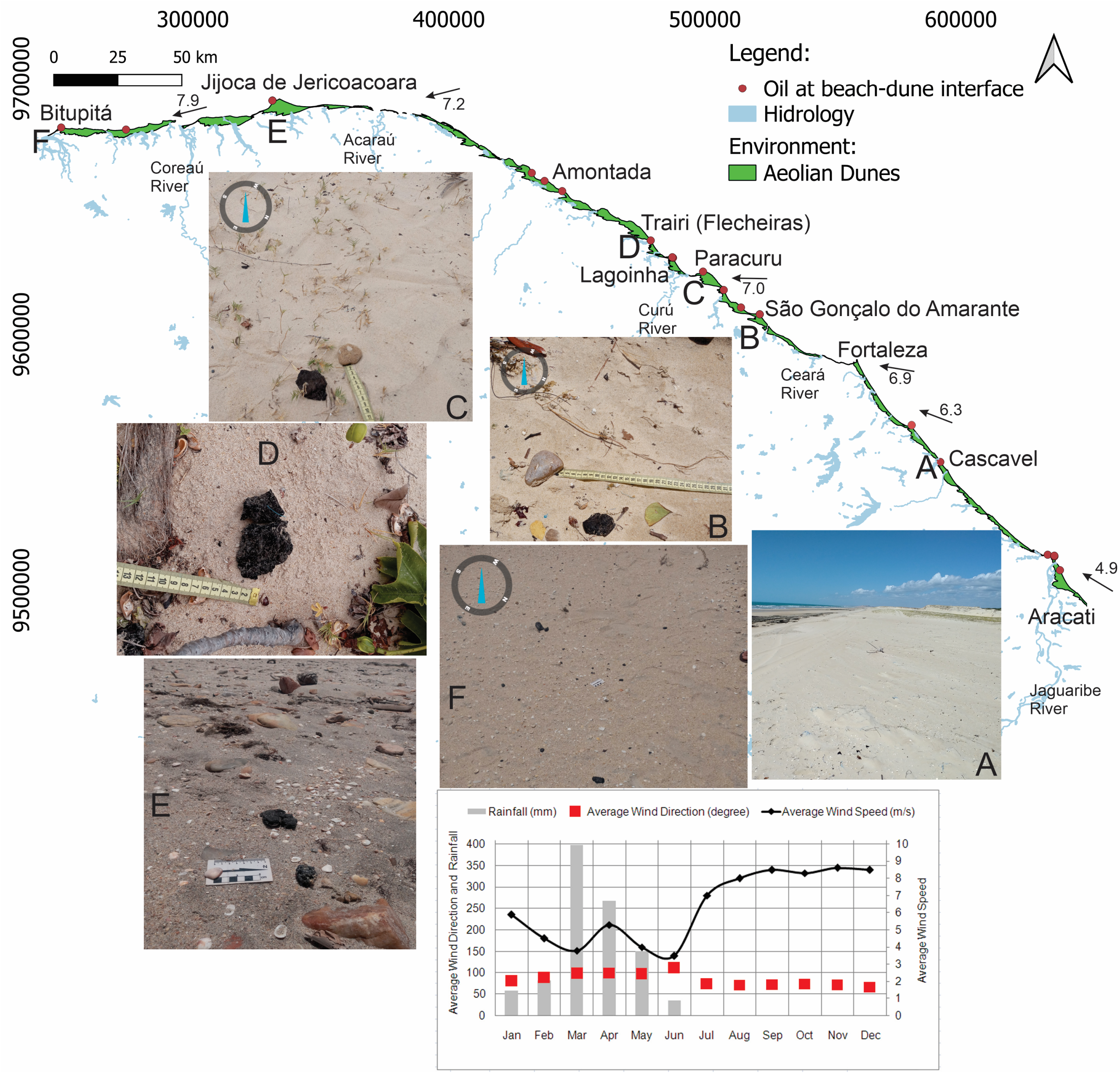

Figure 2. Spatial representation of oil sites at the beach–dune interface on the coast of Ceará after the 2019 oil spill event. Six points (**A**–**F**) are highlighted with photos obtained in the field of the tar balls occurrence. Furthermore, it is noted that the black arrows represent the most frequent wind direction and their respective mean annual velocity (m/s) values [40]. The graph at the bottom illustrates the annual relationship between rainfall, wind direction, and wind speed for Jericoacoara [31].

Oil fragments larger than 50 mm, as well as gravels, are found inland, beyond the upper foreshore and into the backshore (Figure 4), areas, seasonally impacted by storm surges. The oils stranded along these beaches occur as mats, tar balls, and small fragments, generally mixed with sand, which tends to detach as the oil dries.

The incipient foredunes along these stretches are either absent or very low, with sparse vegetation cover, primarily grasses. The leeward surface shows aeolian deflation in some areas, where the Barreiras Formation is exposed, revealing gravels and pebbles.

Figure 3. Area with low incipient foredunes showing aeolian deflation (**A**). Oil fragments appear near the car position (**B**), starting with large fragments over 50 mm immediately after the aeolian crest stretch under deflation (**C**), transitioning to smaller fragments carried by the wind about 20 m from the high tide line (**D**).

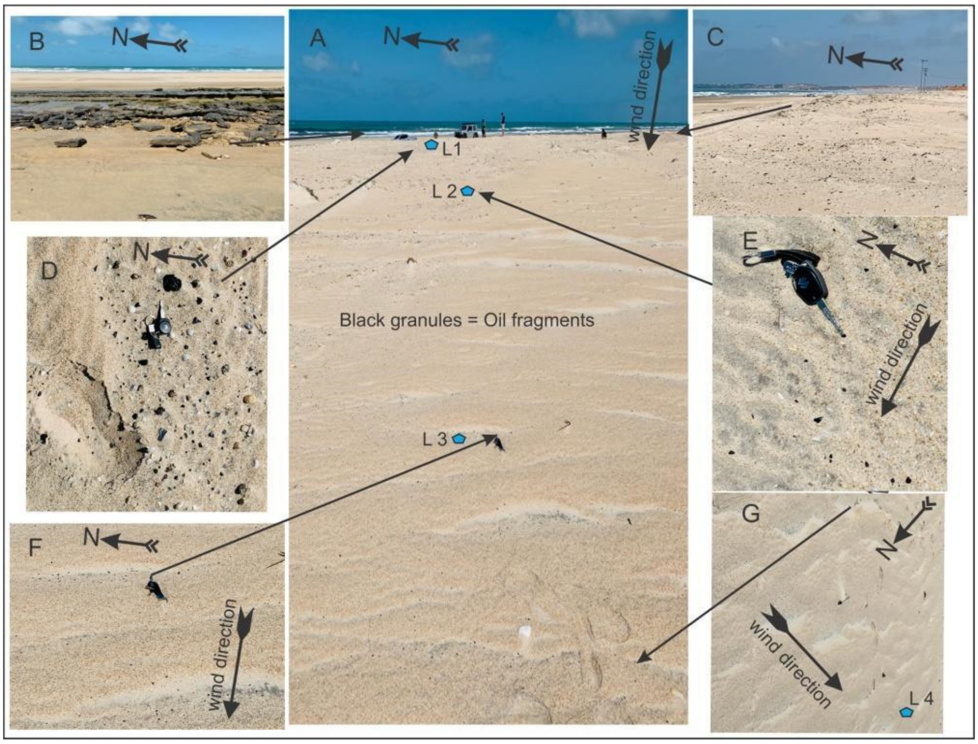

Figure 4. (**A**) Sample positions; (**B**) Beachrock in the middle of the beach profile; (**C**) Incipient foredunes on the east side and minimal foredunes on the west (left of the photo); (**D**) First sampling area with oil fragments (black granules), still under storm surge influence; (**E**) First area of wind transport with oil fragments about 93 m from the high tide line; (**F**) Second area of wind transport with oil fragments around 123 m from the high tide line; (**G**) Area where wind transport causes significant selection and reduction in oil fragment size, about 150 m from the high tide line.

West of the Trairi River mouth (Figure 1), wind-driven oil transport is particularly evident, demonstrating the movement of oil fragments from the beach face, past the incipient foredunes, and more than 100 m inland from the storm surge zone (Figure 4).

In this process, sand ripples form (Figure 4A,E–G), with oil fragments ranging in size from 3 mm to over 50 mm. Larger oil fragments, greater than 50 mm, are concentrated in the upper foreshore and the initial backshore area (Figure 4), which are seasonally impacted by storm surges. These areas contain poorly sorted coarse sand with gravels and shells. As the sediments move inland, the sediment composition shifts to poorly sorted coarse sand with small shells and oil fragments up to 10 mm. As the wind transports the sediments further inland, the fragments become more sorted, and the oil fragment size decreases. First, moderately sorted medium sands contain oil fragments up to 5 mm, then well-sorted medium sands with oil fragments around 3 mm are found farther inland (Table 1).

Table 1. Textural analysis and statistical parameters of the sediments along the coastal stretch between Lagoinha and Flecheiras (Figures 1 and 4), Northeastern Brazil. Legend: MdΦ—median grain size; Si—sediment sorting; Ski—skewness; K—kurtosis.

Samples	MdΦ	Si	Ski	K	Folk & Ward Classification and Oil Description
L 01	1.90	1.32	−0.48	2.65	Poorly sorted coarse sand with gravel, shells and large oil fragments (up to about 50 mm)
L 02	1.78	1.25	−0.14	2.53	Poorly sorted coarse sand with shells and oil fragments (up to about 10 mm)
L 03	1.44	0.72	0.34	0.84	Moderately sorted medium sand with oil fragments (up to about 5 mm)
L 04	1.36	0.41	0.32	1.11	Well-sorted medium sand with oil fragments (up to about 3 mm)

In the coastal section between Lagoinha and Flecheiras, wind direction is predominantly from the ESE, with a secondary influence from the E. In this stretch, wind transport comes from a 93° azimuth direction, with an average speed of 8.61 m/s and a maximum of 9.60 m/s in Flecheiras. These conditions create a high potential for wind transport and subsequent dune formation, as noted by Carvalho [16].

4.2. Coastal Process

The coast of Ceará is clearly marked by seasonality in coastal processes, with the wave climate being characterized by the predominance of Sea waves (<10 s) and secondarily Swell waves (>10 s). In the Jan–Jun period, there is a predominance of waves arriving from the NNE quadrant with low heights (<1 m); however, in Jul–Dec, there is a predominance of waves coming from the E quadrant, with slightly higher average heights (Figure 5). This seasonality is also evident in the wind intensity patterns, in which from Jul–Dec the winds have a higher average speed than at the beginning of the year (Figure 2).

Regarding tidal amplitude, this region is marked by the influence of the mesotidal regime. In Figure 6, we observe the annual variability, in which there is a predominance of amplitudes between 3 and 3.3 m. This factor is fundamental to explain, together with the wave climate and wind speed, the process of migration of oil pellets (or tar balls) to the coastal wind system of Ceará.

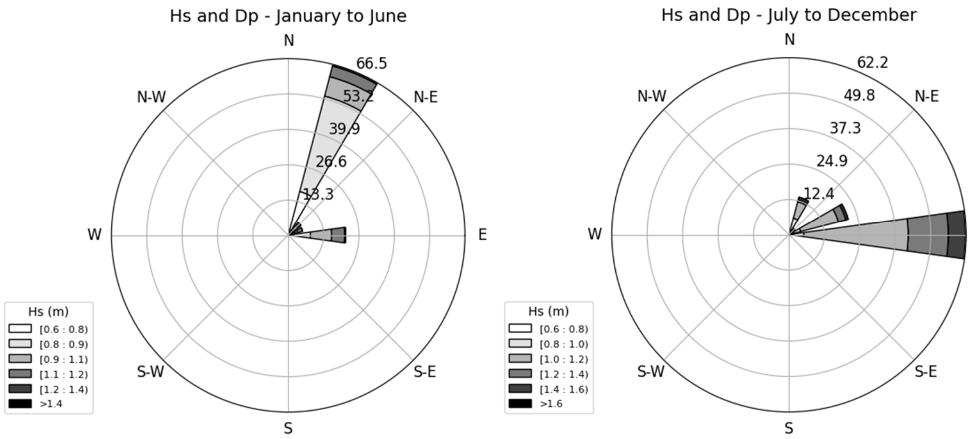

Figure 5. Wave Direction (Dp) and Wave Height (Hs) pattern seasonally represented.

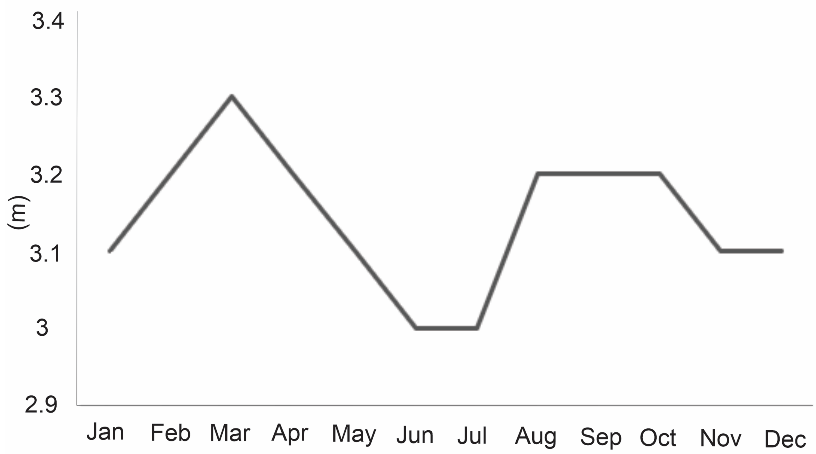

Figure 6. Tidal range represented monthly for the studied area.

Wind patterns are controlled by the seasonal alternation between dry and rainy periods, driven by the migration of the Intertropical Convergence Zone (ITCZ), which is influenced by the convergence of the northeast and southeast trade winds. From December to May, the ITCZ shifts southward, reaching its southernmost position in March and April, bringing increased rainfall and dominant northeast trade winds. From July to November, it gradually moves northward, leading to reduced precipitation and marking the dry season, during which southeast and east trade winds prevail. Wind speeds are highest between August and October and lowest from March to May (Figure 2). El Niño events intensify the dry season by maintaining a more northerly position of the ITCZ. Winds are predominantly from the east (E) and east-southeast (ESE), mainly shaped by the southeast trade winds, and exhibit a unidirectional pattern with high directional consistency (RDP/DP $\approx$ 1) and an average drift potential of approximately 692 v.u. [24].

5. Discussion

The oil that reached the Brazilian coast in 2019 was characterized as a bulk oil, consisting of a mixture of crude oil and fuel-derived residues, according to Reddy et al. [10]. This material persisted in the environment for an extended period and was detected at multiple locations along the coastline, as confirmed by oil fingerprinting analyses [1,17,41]. The oil likely drifted offshore for several days prior to landfall, as indicated by the relative depletion of light and volatile compounds [10].

Comprehensive chemical analyses revealed a complex composition, encompassing multiple classes of hydrocarbons and associated compounds [10]. Saturated hydrocarbons were identified, including n-alkanes (C13–C41), isoprenoids (pristane and phytane), as well as branched and cyclic alkanes. Polycyclic aromatic hydrocarbons (PAHs) ranging from two to six rings were detected, with a predominance of alkylated homologues, consistent with a petrogenic signature. Sulfur-containing aromatics, such as benzothiophenes, dibenzothiophenes, and naphthobenzothiophenes, were also present. In addition, a comprehensive suite of geochemical biomarkers was identified, including hopanes, steranes, diasteranes, triterpanes, and tri- and tetracyclic compounds. Biomarkers indicative of in-reservoir biodegradation, such as 25-norhopanes and 8,14-secohopanes, were detected, together with carotenoid derivatives (e.g., β-carotane and isorenieratane), supporting a marine, anoxic depositional environment [10].

Furthermore, the application of Fourier transform ion cyclotron resonance mass spectrometry (FT-ICR MS) enabled the characterization of high-molecular-weight fractions, including N-, S-, and O-containing species and highly condensed aromatic structures. The relative abundance of high-DBE compounds and extended alkylated series is consistent with thermally altered and residuum-type materials, supporting the interpretation that the spilled oil was not solely a virgin crude but likely included refined or thermally processed components. This approach extended the compositional assessment beyond the GC-amenable fraction and provided additional insight into the oil's thermal history [10].

These oils may have reached the coast mainly by floating, related to transport through currents [42], but also after settling on the seabed and subsequently being carried by swell waves. In this context, the International Maritime Organization (IMO, [43]) relates negative buoyancy to the oil's inherently high density, to density increases caused by weathering or other processes, or to the adhesion of sediments to the spilled oil. Michel and Bambach [44] measured oil density values between 0.87 g/cm^3 and 1.0 g/cm^3 and noted that submerged oil mats (SOMs), which may be classified as oily (>40% oil) or sandy (<40% oil), pose a risk of oil separating from the sand and refloating. Even without drying, these density values are significantly lower than those of wind-transported sediments [45,46], an aspect that indicates a high potential for wind transport of these oil particles.

The local data also suggest that consolidated beach structures (e.g., beachrocks) exposed to oil can retain the material and release its components gradually over extended periods. Consequently, these geological structures may act as latent sources of contamination, posing substantial risks for long-term environmental impact [47]. In this context, wind plays a significant role in dispersing the oil along the coastal zone.

Along the coastal stretches where wind-driven transport of oil fragments was identified, wind transport potential is high, while coastal drift intensity is relatively low—conditions that favor high dune formation [16]. This explains the wind's ability to carry fragments over large distances and suggests that a significant amount of sediment is available on the beach for wind transport. However, the deflation process occurs landward of these stretches, exposing the surface of the Barreiras Formation. This indicates a sediment deficit for wind transport along the beach profile, leading to deflation on the backshore surface or an aeolian erosion fetch effect, similar to that described by Gillette et al. [48].

The intertidal zone is a key source of aeolian sediment [49,50], and there is a strong correlation between aeolian transport and tidal levels (e.g., [41,51]). Beachrock formations along the intertidal zone may act as barriers to wind transport, limiting the volume of sediment available along the beach profile—an essential factor in aeolian transport studies on natural beaches, as noted by Jackson and Cooper [52]. Beachrock platforms can also interfere with or reduce fetch effects, as observed by Nordstrom and Jackson [53]; Davidson-Arnott et al. [54]; Bauer and Davidson-Arnott [55]; and Davidson-Arnott and Bauer [56].

Moreover, Beachrock structures may facilitate the retention of oil between the Beachrock and the upper beach profile (Figure 7). This entrapment can promote the drying and fragmentation of the oil, making it easier for wind to transport the fragments. Wind selection, wind-driven fragmentation, or both processes likely reduce the size of oil particles, allowing them to become fully integrated into the aeolian environment. These fragments may contribute to dune pollution and potentially move into lakes, rivers, or estuarine systems, as dunes frequently intercept these environments. Such oil presence, if highly concentrated, may be disruptive to certain biological cycles or interfere in trophic chains [57]. Notably, the presence of oil in inland areas influenced by wind transport was predominantly observed on tide-modified beaches in a morphodynamic state [58].

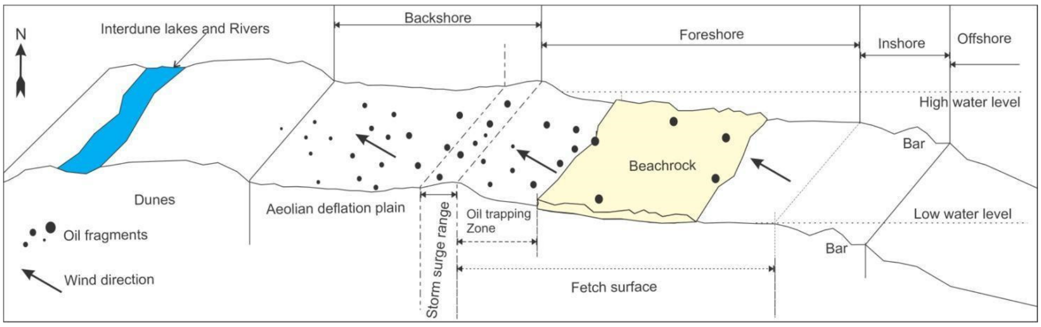

Figure 7. Schematic beach profile showing the locations where oil fragments were found, along with the limitations of the fetch surface under wind action.

6. Conclusions

Fragmentation processes and the wind-driven transport of oil over relatively large distances inland have been identified. So, the wind transport has the potential to carry oil fragments, allowing them to become part of the wind environment and be transferred to other areas, particularly lakes and rivers. These various morphologies, from headlands to beachrocks, influence the likelihood of sediment transport by wind from the beach inland, either facilitating or hindering the movement of different materials.

The presence of beachrocks in the intermediate section of the beach profile can help retain oil in the upper portion of the beach, leading to its drying and rapid fragmentation. Furthermore, the absence or low height of incipient foredunes can facilitate the migration of oil from the beach into inland areas.

This underscores the potential of aeolian processes to contribute to the contamination caused by these oil fragments in wind-driven and interconnected environments, as well as the risk of contaminating the organisms living in these ecosystems.

Author Contributions: Conceptualization, A.M.d.C., L.d.S.P., A.R.X.N. and R.M.C.; methodology, A.M.d.C., L.d.S.P., A.R.X.N., V.C.-S., S.R., J.F.S.L.J., R.P.L.F., B.D.L., T.d.S.S. and R.M.C.; investigation, A.M.d.C., L.d.S.P., A.R.X.N. and R.M.C.; writing—original draft preparation, A.M.d.C., L.d.S.P., A.R.X.N. and R.M.C.; writing—review and editing, A.M.d.C., L.d.S.P., A.R.X.N., V.C.-S., S.R. and R.M.C.; visualization, A.M.d.C., L.d.S.P., A.R.X.N., V.C.-S., S.R., J.F.S.L.J., R.P.L.F., B.D.L., T.d.S.S. and R.M.C.; supervision, L.d.S.P. and R.M.C.; funding acquisition, R.M.C. All authors have read and agreed to the published version of the manuscript.

Funding: This research was funded by Dispersants and adsorbents for remediation of coastal areas affected by crude oil spills (Coast of Ceará, Northeast Brazil) (440868/2020–3).

Data Availability Statement: The original contributions presented in this study are included in the article. Further inquiries can be directed to the corresponding author.

Acknowledgments: Instituto de Ciências do Mar-LABOMAR-UFC; and FUNCAP. R. M. Cavalcante, L. d. S. Pinheiro and S. Rossi are grateful for the PQ Grant (314013/2023-7-CNPq, 305401/2025-4 CNPq, 314460/2023-3-Cnpq), CAPES-PRINT (Finance code 001), and Assessment of the oil spill

(2019/2020) on the semi-arid coast of Brazil (440880/2020- 3), INCT-AmbTropic phase II (CNPq Process 465634/2014-1), and project "Dispersants and adsorbents for remediation of coastal areas affected by crude oil spills (Coast of Ceará, Northeast Brazil)" (440868/2020–3), both linked to MCTI Emergency Action to Combat the Oil Spill (2020), as well as Lemae/Finep/CNPq (380975/2022–0) and Secretaria do Meio Ambiente e Mudança do Clima (SEMA/CE) for providing the vehicle for the study.

Conflicts of Interest: The authors declare no conflict of interest.

References

1. Al-Yakoob, S.; Saeed, T.; Al-Hashash, H. Polycyclic aromatic hydrocarbons in edible tissue of fish from the Gulf after the 1991 oil spill. *Mar. Pollut. Bull.* **1993**, *27*, 297–301. [CrossRef]
2. Rumney, H.S.; Laruelle, F.; Potter, K.; Mellor, P.K.; Law, R.J. Polycyclic aromatic hydrocarbons in commercial fish and lobsters from the coastal waters of Madagascar following an oil spill in August 2009. *Mar. Pollut. Bull.* **2011**, *62*, 2859–2862. [CrossRef]
3. Rumney, H.S.; Potter, K.; Mellor, P.K.; Brant, J.; Whomersley, P.; Shaw, S.; Barry, J.; Kirby, M.F.; Law, R.J. Polycyclic aromatic hydrocarbons in fish from St Helena, South Atlantic, in relation to an historic wreck. *Mar. Pollut. Bull.* **2014**, *89*, 451–454. [CrossRef]
4. Soares, M.O.; Teixeira, C.E.P.; Bezerra, L.E.A.; Rossi, S.; Tavares, T.C.L.; Cavalcante, R.M. Brazil oil spill response: Time for coordination. *Science* **2020**, *367*, 155. [CrossRef]
5. Yang, Z.K.; Shah, K.; Laforest, S.; Hollebone, B.P.; Situ, J.; Crevier, C.; Lambert, P.; Brown, C.E.; Yang, C. Occurrence and weathering of petroleum hydrocarbons deposited on the shorline of the North Saskatchewan River from the 2016 Husky oil spill. *Environ. Pollut.* **2020**, *258*, 113769. [CrossRef]
6. Uno, S.; Koyama, J.; Kokushi, E.; Monteclaro, H.; Santander, S.; Cheikyula, J.O.; Miki, S.; Añasco, N.; Pahila, I.G.; Taberna, H.S.; et al. Monitoring of PAHs and alkylated PAHs in aquatic organisms after 1 month from the Solar I oil spill off the coast of Guimaras Island, Philippines Environ. *Monit. Assess.* **2010**, *165*, 501–515. [CrossRef]
7. Cavalcante, R.M.; Lima, A.D.F.; de Souza Abessa, D.M.; de Alkimin, G.D.; Santana, L.M.B.M.; Mello, L.C.; Soares, M.O. Oil Spill Impacts on Marine Food Webs: Lessons From Contamination in Tropical Coasts. In *Treatise on Estuarine and Coastal Science*, 2nd ed.; Baird, D., Elliott, M., Eds.; Elsevier: Oxford, UK, 2024; Volume 4, pp. 706–734. [CrossRef]
8. Soares, M.O.; Teixeira, C.E.P.; Bezerra, L.E.A.; Paiva, S.V.; Tavares, T.C.L.; Garcia, T.M.; Araujo, J.T.; Campos, C.C.; Ferreira, S.M.C.; Matthews-Cascon, H.; et al. Oil spill in South Atlantic (Brazil): Environmental and governamental disaster. *Mar. Policy* **2020**, *115*, 103879. [CrossRef]
9. Soares, M.O.; Teixeira, C.E.P.; Luis Ernesto Arruda Bezerra, L.E.A.; Rabelo, E.F.; Castro, I.B.; Cavalcante, R.M. The most extensive oil spill registered in tropical oceans (Brazil): The balance sheet of a disaster. *Environ. Sci. Pollut. Res.* **2022**, *29*, 19869–19877. [CrossRef]
10. Reddy, C.M.; Nelson, R.K.; Hanke, U.M.; Cui, X.; Summons, R.E.; Valentine, D.L.; Rodgers, R.P.; Chacón-Patiño, M.L.; Niles, S.F.; Teixeira, C.E.P.; et al. Synergy of Analytical Approaches Enables a Robust Assessment of the Brazil Mystery Oil Spill. *Energy Fuel.* **2022**, *36*, 13688–13704. [CrossRef]
11. Mello, L.C.; Nascimento, A.P.; Lopes, B.D.; Lima, A.D.; Bezerra, L.E.; Mendes, L.d.F.; Bastos, L.M.; Nossol, A.B.; Martins, M.M.; Martins, L.L.; et al. Tarballs on the Brazilian coast in late 2022 sustain Lepas anatifera Linnaeus, 1758 (Crustacea: Cirripedia): Occurrence and risk of petroleum hydrocarbon ingestion. *Sci. Total Environ.* **2023**, *896*, 164981. [CrossRef] [PubMed]
12. Lessa, G.C.; Teixeira, C.E.P.; Pereira, J.; Santos, M.F. The 2019 Brazilian oil spill: Insights on the physics behind the drift. *J. Mar. Syst.* **2021**, *222*, 103586. [CrossRef]
13. IPIECA/IOGP. *Impacts of Oil Spills on Shorelines: Good Practice Guidelines for Incident Management and Emergency Response Personnel*; IOGP Report 534; The Global Oil and Gas Industry Association for Environmental and Social Issues: London, UK, 2016; 56p.
14. Köppen, W. Das geographische System der Klimate. In *Handbuch der Klimatologie*; Köppen, W., Geiger, R., Eds.; Gerbrüder Borntraeger: Berlin, Germany, 1936; Volume I, 44p.
15. IPECE. *Perfil Municipal 2017*; Ano I—Janeiro de 2018; Instituto de Pesquisa e Estratégia Econômica do Ceará—IPECE: Fortaleza, Brazil, 2018.
16. Carvalho, A.M. Dinâmica Costeira Entre Cumbuco e Matões-Costa NW do Estado do Ceará. Ênfase Nos Processos Eólicos. Ph.D. Dissertation, Universidade Federal da Bahia, UFBA, Salvador, Brazil, 2003; 188p.
17. Maia, L.P. Procesos Costeros y Balance Sedimentario a lo Largo de Fortaleza (NE-Brasil): Implicaciones Para Una Gestión Adecuada de la Zona Litoral. Ph.D. Dissertation, Universitat de Barcelona, Barcelona, Spain, 1998.
18. Morais, J.O. Aspectos do transporte de sedimentos no litoral do município de Fortaleza, Estado do Ceará, Brasil. *Arq. Ciências Mar* **1980**, *20*, 71–100.

19. Eduardo, L.M.; Carvalho, A.M.; Lima Júnior, S.B.; Claudino-Sales, V.; Gastão, F.G.C.; Castelo Branco, J.L.; Pinheiro, L.S. Using Direct and Indirect Methods to Assess the Influence of High-Energy Waves over Beach Sedimentary Balance (Brazilian Northeastern Region). *J. Coast. Res.* **2021**, *37*, 1235–1246. [CrossRef]
20. Claudino-Sales, V. Cenários Litorâneos—Lagoa do Papicu, Natureza e Ambiente na Cidade de Fortaleza, Ceará. Master's Thesis, Universidade Federal de São Paulo, USP, São Paulo, Brazil, 1993; 349p.
21. Claudino-Sales, V.; Wang, P.; Carvalho, A.M. Interactions between various headlands, beaches and dunes along the coast of Ceará State, Northeast Brazil. *J. Coast. Res.* **2018**, *34*, 413–428. [CrossRef]
22. Chung, J.C. Correlations between the tropical Atlantic trade winds and precipitation in northeastern Brazil. *J. Climatol.* **1982**, *2*, 35–46. [CrossRef]
23. Utida, G.; Cruz, F.W.; Etourneau, J.; Bouloubassi, I.; Schefub, E.; Vuille, M.; Novello, V.F.; Prado, L.F.; Sifeddine, A.; Klein, V.; et al. Tropical South Atlantic influence on Northeastern Brazil precipitation and ITCZ displacement during the past 2300 years. *Sci. Rep.* **2019**, *9*, 1698. [CrossRef]
24. Tsoar, H.; Levin, N.; Porat, N.; Maia, L.P.; Herrmann, H.J.; Tatumi, S.H.; Claudino-Sales, V. The effect of climate change on the mobility and stability of coastal sand dunes in Ceará State (NE Brazil). *Quat. Res.* **2009**, *71*, 217–226. [CrossRef]
25. Fisch, C.L. Caracterização do Clima de Ondas na Costa do Ceará. Master's Thesis, Universidade Federal do Rio de Janeiro, Rio de Janeiro, Brazil, 2008; 231p.
26. Mendes, D.; Mendes, M.D. Climatology of cyclones, anticyclones and storm tracks: Revision of concepts. *Rev. Bras. Geofísica* **2004**, *22*, 127–134. [CrossRef]
27. Trigo, I.F.; Davies, T.D.; Bigg, G.R. Objective climatology of cyclones in the Mediterranean region. *J. Clim.* **1999**, *12*, 1685–1696. [CrossRef]
28. Farias, E.G.G. Uso de Dados Obtidos Por Sensores Orbitais Ativos no Estudo Dos Campos de Ondas de Superfície no Atlântico Norte Tropical. Ph.D. Dissertation, Instituto Nacional de Pesquisas Espaciais (INPE), São José dos Campos, Brazil, 2012; 207p.
29. Hesp, P.A.; Maia, L.M.; Claudino-Sales, V. The Holocene barriers of Maranhão, Piauí and Ceará States, Northeastern Brazil. In *Geology of the Brazilian Coastal Barriers*; Lecture Notes in Earth Sciences; Dillenburg, S.R., Hesp, P., Eds.; Springer: Berlin, Germany, 2009; pp. 325–345.
30. Yasso, W.E. Plan geometry of headland-bay beaches. *J. Geol.* **1965**, *73*, 702–719. [CrossRef]
31. Carvalho, A.M.; Ellis, J.T.; Lamothe, M.; Maia, L.M. Using Wind Direction and Shoreline Morphology to Model Sand Dune Mobilization. *J. Coast. Res.* **2016**, *32*, 1005–1015. [CrossRef]
32. Hsu, J.R.C.; Uda, T.; Silvester, R. Beach downcoast of harbours in bays. *Coast. Eng.* **1993**, *19*, 163–181. [CrossRef]
33. Ximenes Neto, A.R.; da Silva, R.R.; de Paula, D.P.; Leisner, M.M.; Cordeiro, A.M.N.; de Morais, J.O.; Pinheiro, L.D.S. Spatial distribution and deposits of cliffs along the Brazilian semi-arid coast. *Geomorphology* **2024**, *466*, 109451. [CrossRef]
34. Pye, K.; Tsoar, H. *Aeolian Sand and Sand Dunes*; Springer: Berlin/Heidelberg, Germany, 2009.
35. Allmendinger, R.W. Stereonet Mobile 10 for IOS. 2006. Available online: https://rickallmendinger.net (accessed on 3 February 2020).
36. Suguio, K. *Introdução à Sedimentologia*; EDUSP: São Paulo, Brazil, 1973; 317p.
37. Wentworth, C.K. A scale of grade and class terms for clastic sediments. *J. Geol.* **1922**, *30*, 377–392. [CrossRef]
38. Camargo, M.G. Sysgran: Um sistema de código aberto para análises granulométricas do sedimento. *Rev. Bras. Geociências* **2006**, *36*, 371–378. [CrossRef]
39. Folk, R.L.; Ward, W.C. Brazos River bar [Texas]; A study in the significance of grain size parameters. *J. Sediment. Petrol.* **1957**, *27*, 3–26. [CrossRef]
40. Jiménez, J.A.; Maia, L.P.; Serra, J.; Morais, J. Aeolian dune migration along the Ceará coast, northeastern Brazil. *Sedimentology* **1999**, *46*, 689–701. [CrossRef]
41. De Vries, S.; Arens, S.M.; Stive, M.J.F.; Ranasinghe, R. Dune growth trends and the effect of beach width on annual timescales. In *Proceedings of Coastal Sediments, Miami, FL, USA, 2–6 May 2011*; World Scientific: Singapore, 2011; pp. 712–724.
42. Zacharias, D.C.; Crespo, N.M.; da Silva, N.P.; da Rocha, R.P.; Gama, C.M.; e Silva, S.B.R.; Harari, J. Oil reaching the coast: Is Brazil on the route of international oceanic dumping? *Mar. Pollut. Bull.* **2023**, *196*, 115624. [CrossRef] [PubMed]
43. International Maritime Organization. *Operational Guidelines on Sunken and Submerged Oil Assessment and Removal Techniques*; International Maritime Organization: London, UK, 2016. Available online: https://imo-epublications.org/content/books/9789280115895 (accessed on 23 December 2024).
44. Michel, J.; Bambach, P. A response guide for sunken oil mats (SOMs): Formation, behavior, detection, and recovery. *J. Mar. Sci. Eng.* **2022**, *10*, 368. [CrossRef]
45. Huang, N.; Zheng, X.J.; Zhou, Y.-H.; Van Pelt, R.S. Simulation of wind-blown sand movement and probability density function of liftoff velocities of sand particles. *J. Geophys. Res.* **2006**, *111*, D20201. [CrossRef]
46. Kamath, S.; Parteli, E. Toward a large-scale particle-based parallel simulator of Aeolian sand transport, including a model for mobile sand availability. *EPJ Web Conf.* **2021**, *249*, 13004. [CrossRef]

47. Ximenes Neto, A.R.; Pinheiro, L.; Carvalho, A.M.; Rossi, S.; Júnior, J.F.S.L.; Filho, R.P.L.; Lopes, B.D.; Sousa, T.S.; Nascimento, A.P.; Martins, L.L.; et al. Beachrocks in Oil-Contaminated Areas: Reservoirs and Potential Sources of Environmental Pollution. *Mar. Pollut. Bull.* **2025**. *submitted*.
48. Gillette, D.A.; Herbert, G.; Stockton, P.H.; Owen, P.R. Causes of the fetch effect in wind erosion. *Earth Surf. Process. Landf.* **1996**, *21*, 641–659. [CrossRef]
49. Houser, C. Synchronization of transport and supply in beach-dune interaction. *Prog. Phys. Geogr.* **2009**, *33*, 733–746. [CrossRef]
50. Hoonhout, B.; De Vries, S.; Cohn, N. The influence of spatially varying supply on coastal aeolian transport: A field experiment. Coastal Sediments. In *Proceedings of the Coastal Sediments, San Diego, CA, USA, 11–15 May 2015*; World Scientific: Singapore, 2015; pp. 11–15.
51. Arens, S.M. Rates of aeolian transport on a beach in a temperate humid climate. *Geomorphology* **1996**, *17*, 3–18. [CrossRef]
52. Jackson, D.W.T.; Cooper, J.A.G. Beach fetch distance and aeolian sediment transport. *Sedimentology* **1999**, *46*, 517–522. [CrossRef]
53. Nordstrom, K.F.; Jackson, N.L. Effect of source width and tidal elevation changes on aeolian transport on an estuarine beach. *Sedimentology* **1992**, *39*, 769–778. [CrossRef]
54. Davidson-Arnott, R.G.D.; MacQuarrie, K.; Aagaard, T. The effects of wind gusts, moisture content and fetch length on sand transport on a beach. *Geomorphology* **2005**, *68*, 115–129. [CrossRef]
55. Bauer, B.O.; Davidson-Arnott, R.G.D. A general framework for modeling sediment supply to coastal dunes including wind angle, beach geometry, and fetch effects. *Geomorphology* **2002**, *49*, 89–108. [CrossRef]
56. Davidson-Arnott, R.G.D.; Bauer, B.O. Controls on the geomorphic response of beach-dune systems to water level rise. *J. Great Lakes Res.* **2021**, *47*, 1594–1612. [CrossRef]
57. Dupuis, A.; Ucan-Marin, F. A literature review on the aquatic toxicology of petroleum oil: An overview of oil properties and effects to aquatic biota. In *DFO Canadian Science Advisory Secretariat Research Document*; 2015/007; Fisheries and Oceans Canada: Ottawa, ON, Canada, 2025; vi + 52 p.
58. Pinheiro, L.S.; Morais, J.O.; Maia, L.P. The Beaches of Ceará. In *Brazilian Beach Systems*; Coastal Research Library; Short, A., Klein, A., Eds.; Springer: Cham, Switzerland, 2016; Volume 17. [CrossRef]